Modeling Earth Albedo Currents on Sun Sensors for Improved Vector Observation.

Dan D. V. Bhanderi *

Aalborg University, Fredrik Bajers Vej 7C, DK-9220 Aalborg Oest, Denmark

Earth albedo influences vector measurements of the solar line of sight vector, due to the induced current on in the photo voltaics of Sun sensors. Although advanced digital Sun sensors exist, these are typically expensive and may not be suited for satellites in the nano or pico-class. Previously an Earth albedo model, based on reflectivity data from NASA's Total Ozone Mapping Spectrometer project, has been published. In this paper the proposed model is presented, and the model is sought validated by comparing simulated data with telemetry from the Danish Ørsted satellite. A novel method for modeling Sun sensor output by incorporating the Earth albedo model is presented. This model utilizes the directional information of in the Earth albedo model, which is achieved by Earth surface partitioning. This allows accurate simulation of the Sun sensor output and the results are consistent with Ørsted data, showing significant improvement in the Earth albedo induced current estimates. Additionally an algorithm for utilizing the Earth albedo model in obtaining a vector observation pair which is superior to the solar line of sight vector pair. It is concluded that the Earth albedo model is valid and useful for space environment simulations, and may be utilized to improve attitude estimation algorithms applying Sun sensor vector observations.

Nomenclature

A_c = Cell area
$\boldsymbol{A}_I^B$ = Attitude matrix of frame B relative to frame I
α_{irad} = Angle of incident irradiance
α_{sat} = Angle to satellite from grid point
α_{Sun} = Angle of incident irradiance on cell
$\boldsymbol{D}$ = Set of grid points
$\Delta\phi_g$ = Angular resolution in latitude
$\Delta\theta_g$ = Angular resolution in longitude
$\boldsymbol{\Phi}$ = Set of latitude grid points
E_a = Total Earth albedo
E_{AM0} = Incident air mass zero solar irradiance at 1AU
E_c = Cell albedo irradiance
E_{cal} = Incident irradiance during calibration of Sun sensors
E_{irad} = Incident irradiance
ϕ_g = Polar angle of grid point
i_{max} = Maximum Sun sensor current during calibration of Sun sensors
i_{meas} = Measured Sun sensor current
j = Counter variable
L = Loss function
n = Number of vector observations
$\hat{\boldsymbol{n}}_c$ = Cell normal vector
$\hat{\boldsymbol{n}}_{SS}$ = Sun sensor normal vector

*Assistant Professor, Department of Control Engineering.

$\boldsymbol{r}_{\mathrm{g}}$ = Position of grid point relative to solar cell center
$\boldsymbol{r}_{\mathrm{E}}$ = Nadir vector
$\boldsymbol{r}_{\mathrm{src}}$ = Vector to irradiance source
$\boldsymbol{r}_{\mathrm{sat}}$ = Satellite position vector
$\boldsymbol{r}_{\mathrm{Sun}}$ = Sun position vector
$\boldsymbol{r}_{\mathrm{SunEst}}$ = Estimated Sun position vector
ρ = Reflectivity
$\boldsymbol{\Theta}$ = Set of longitude grid points
θ_{g} = Azimuth angle of grid point
$\boldsymbol{V}_{\mathrm{sat}}$ = Set of grid points in satellite FOV
$\boldsymbol{V}_{\mathrm{Sun}}$ = Set of sunlit grid points
$\boldsymbol{v}$ = Vector
w = Weight parameter

I. Introduction

Sun sensors are widely used on-board satellites for attitude determination. Sun sensors are used to obtain a vector measurement of the Sun in a spacecraft-fixed frame, which is compared to ephemeris models to obtain the same vector in an inertial frame. Combined with other vector measurements, an attitude of the spacecraft-fixed frame with respect to the inertial frame, is obtained. Sun sensors measure the incoming solar irradiance. These measurements are perturbed by the sunlight reflected by Earth, known as the Earth albedo. The Earth albedo influences the power generated by solar panels, generates radiation torques, affects the thermal design, and is utilized by horizon sensors to estimate satellite attitude.[1–3] On analogue Sun sensors Earth albedo generates excess current in the photo voltaics, thus perturbing the Sun vector measurement. Additionally, Earth albedo induces current in solar panels, which can be utilized by the electrical power system in order to increase power generation on the satellite platform. In order to include this in the design phase of the satellite development, accurate models of the Earth albedo are required.

Sun sensors can be divided into two categories, analogue Sun sensors, which simply measure an angle of the incident solar irradiance, and digital Sun sensors, which utilize more sophisticated methods to measure solar angles from the incoming irradiance. Digital Sun sensors are mostly insensitive to albedo light by implementing an active pixel array instead of solar cells.[4] Some configurations result in errors in the least significant bits of the digital Sun sensors.[5] Other methods simply rely on protection of stray light in the sensor hardware.[6] Analogue Sun sensors are very simple and cheap to use, and have been applied on the Danish Ørsted satellite. The same configuration will be used on the AAUSAT-II student satellite, which is a Cubesat, i.e. a pico-satellite, which limits the total mass of the satellite to 1kg. This excludes the possibility of utilizing digital sun sensors and stray light protection strategies, hence the Sun sensors are sensitive to albedo disturbances.

Albedo is typically treated as noise to the Attitude Determination System (ADS). The albedo disturbance is either filtered out statistically in Kalman algorithms,[7,8] which is possible when used with magnetometers, or it can be measured using albedo sensors.[9] A model of the Earth albedo based on the Total Ozone Mapping Spectrometer (TOMS) reflectivity data was published in ([10]). In this paper a model of the Sun sensor currents, which includes the Earth albedo model, is presented. The modeling results are compared to the telemetry data from the Ørsted satellite, in order to validate the albedo modeling. In addition, an algorithm for handling Earth albedo currents in vector based attitude determination is presented. The results of the improved Sun sensor vector observation are calculated from the Ørsted telemetry, and compared to the ephemeris models, based on the attitude measurements from the on-board star tracker, which allows for 20arcsec precision in the attitude reference.[11]

Section II gives a short introduction to the Earth albedo model published in ([10]). The output of the Earth albedo model is used in the calculation of the Sun sensor output currents, presented in Section III. Section IV presents a method for handling Earth albedo currents in the Sun sensor measurements using the QUEST algorithm for attitude determination. The results of the Sun sensor modeling and attitude determination algorithm is presented in Section V, where Ørsted telemetry is applied for reference.

II. Albedo Model

The modeling of the Earth albedo is based on the reflectivity data, measured by the Earth Probe satellite for the TOMS project. The satellite data are given in a resolution of $\Delta\phi_g = 1$deg latitude times $\Delta\theta_g = 1.25$deg longitude, i.e. 180×288 data points. The 2D data space $\boldsymbol{D}$ is defined as a grid of data points $\boldsymbol{\Phi} \times \boldsymbol{\Theta}$, where

$$\boldsymbol{\Phi} = [-89.5\text{deg}, -89.5\text{deg} + \Delta\phi_g, -89.5\text{deg} + 2\Delta\phi_g, ..., -89.5\text{deg} + 179\Delta\phi_g], \quad (1)$$

$$\boldsymbol{\Theta} = [-179.375\text{deg}, -179.375\text{deg} + \Delta\theta_g, -179.375\text{deg} + 2\Delta\theta_g, ..., -179.375\text{deg} + 287\Delta\theta_g]. \quad (2)$$

Each data point $(\phi_g, \theta_g) \in \boldsymbol{D}$ is the mean reflectance of a cell, $\phi_g \pm \Delta\phi_g/2$ and $\theta_g \pm \Delta\theta_g/2$, on the Earth surface. The data point $(-89.5\text{deg}, -179.375\text{deg})$ corresponds to 89.5° South and −179.375° West.

The principle of the modeling scheme is outlined in Fig. 1. The incident solar irradiance E_{AM0} reaches the cell at grid point (ϕ_g, θ_g), at an incident angle of α_{Sun} to the cell normal $\hat{\boldsymbol{n}}_c$. The angle of incidence defines the density of the incident irradiance on the cell. The subscript AM0 states that the irradiance has passed through zero air mass,[12] which is assumed. The amount of radiant flux reflected by the cell is given by the incident irradiance, the reflectivity $\rho(\phi_g, \theta_g)$, of the cell surface, and the area of the cell, $A_c(\phi_g)$. The reflection on the Earth surface is assumed to be Lambertian. Lambertian surfaces have a diffuse reflection, which is independent on the incident angle of the incoming radiance, and look evenly illuminated regardless of the viewing angle.[13] The Earth albedo contribution of the cell, E_c, reaches the satellite, and the density of the radiant flux is dependent on the angle α_{sat} and the distance of the satellite from the grid point.

The incident AM0 solar irradiance is modeled by a black body spectrum with a surface temperature of $5777K$ ([3]) at a distance of 1AU. It may be assumed that the Earth albedo spectrum has the same distribution as the AM0 irradiance.[3] The Earth absorbed solar irradiance, which is radiated back into space as thermal infrared, is not included in the model, since a typical solar cell does not absorb radiance at wavelengths longer than 2μm, see e.g. ([14]). The Earth radiance, modeled as a 288K black body spectrum model, peaks at 10μm and less than $4 \cdot 10^{-80}\%$ of the energy is at wavelengths shorter than 2μm.

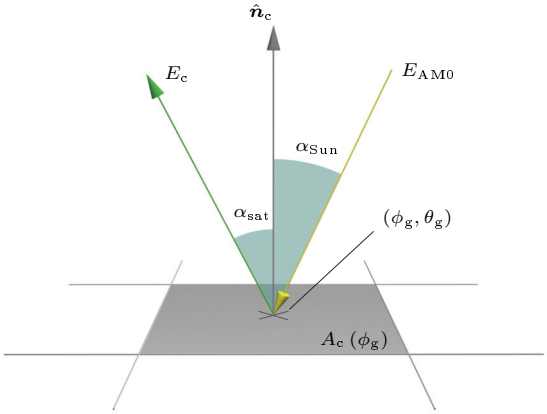

Figure 1. Earth albedo modeling principle. The incoming solar AM0 irradiance is reflected by a cell of the Earth partitioning.

The Earth albedo irradiance $E_c(\phi_g, \theta_g)$ from a single cell, is given by[10]

$$E_c(\phi_g, \theta_g) = \begin{cases} \frac{\rho(\phi_g,\theta_g) E_{\text{AM0}} A_c(\phi_g) \hat{\boldsymbol{r}}_{\text{Sun}}^{\text{T}} \hat{\boldsymbol{n}}_c \hat{\boldsymbol{r}}_{\text{sat}}^{\text{T}} \hat{\boldsymbol{n}}_c}{\pi ||\boldsymbol{r}_{\text{sat}}||^2} & \text{if } (\phi_g, \theta_g) \in \boldsymbol{V}_{\text{Sun}} \cap \boldsymbol{V}_{\text{sat}} \\ 0 & \text{else} \end{cases}, \quad (3)$$

where $\boldsymbol{r}_{\text{Sun}}$ and $\boldsymbol{r}_{\text{sat}}$ denotes the position vectors of the Sun and satellite relative to the grid center. The $\hat{}$ notation implies that normalized vectors are used. The sets $\boldsymbol{V}_{\text{Sun}} \subset \boldsymbol{D}$ and $\boldsymbol{V}_{\text{sat}} \subset \boldsymbol{D}$ are the grid points visible from the Sun and satellite, respectively, i.e. $\boldsymbol{V}_{\text{Sun}} \cap \boldsymbol{V}_{\text{Sun}}$ is the set of sunlit grid points visible from the satellite, which is a necessary conditions for a cell to reflect solar irradiance to the satellite. Note that the vectors $\hat{\boldsymbol{n}}_c$, $\boldsymbol{r}_{\text{Sun}}$, and $\boldsymbol{r}_{\text{sat}}$ are functions of ϕ_g and θ_g.

The output of the albedo model is $E_{\mathrm{c}}(\phi_{\mathrm{g}}, \theta_{\mathrm{g}})$ from the cells at all grid points, i.e. a 180×288 matrix. This result allows for incident angular dependency, when calculating the generated current in photo voltaics as a function of incident irradiance. This modeling is presented in the following section.

III. Sun Sensor Model

The Sun sensor current model is used to calculate the output currents of analogue Sun sensors. Different types of Sun sensors exist. A simple analogue Sun sensor consist of a small solar cell in short circuit mode. Sun sensors of this type are very cheap and small, compared to more advanced sensors, and are suitable for pico-satellite applications. Driving the Sun sensors in short circuit mode, ensures that the current output is dependent mainly on the incoming irradiance. The solar cells used for charging batteries on a satellite, can experience change in current output as a result of high loads. Consequently, using these solar cells requires modeling of the entire electrical system in the satellite, which is very complex. The model derived in this section applies for simple Sun sensors with solar cells in short circuit mode.

The density of the incident irradiance is clearly dependent on the angle of the incident irradiance, since the density of the radiant flux on the solar cell surface in the Sun sensor changes with this parameter. From the density of the radiant flux on the Sun sensor, the output current may be calculated from the area and efficiency of the solar cell. Typically, the Sun sensor is calibrated on-ground, by illuminating the Sun sensors with a known irradiance, denoted E_{cal}, and measuring the current output, $i_{\max}$, when the angle of incidence is zero, i.e. the irradiance is perpendicular on the solar cell plane. The measured current from an ideal Sun sensor j, as a function of the angle of incidence $\alpha_{\mathrm{irad},j}$, is expressed as

$$i_{\mathrm{meas},j} = i_{\max,j} \cos\left(\{\alpha_{\mathrm{irad},j}\}_{-\infty}^{\pi/2}\right). \tag{4}$$

The angle $\alpha_{\mathrm{irad},j}$ is measured as the angle between the normal vector to the Sun sensor solar cell plane, $\hat{\boldsymbol{n}}_{\mathrm{SS},j}$, and the Line of Sight (LOS) vector to the irradiance source, $\hat{\boldsymbol{r}}_{\mathrm{src}}$, illustrated in Fig. 2. The notation $\{\cdot\}_{-\infty}^{\pi/2}$ indicates that the angle of the incident irradiance saturates at $\pi/2$. When the angle of incidence exceeds $\pi/2$ the Sun sensor is illuminated from the back, hence no current is generated.

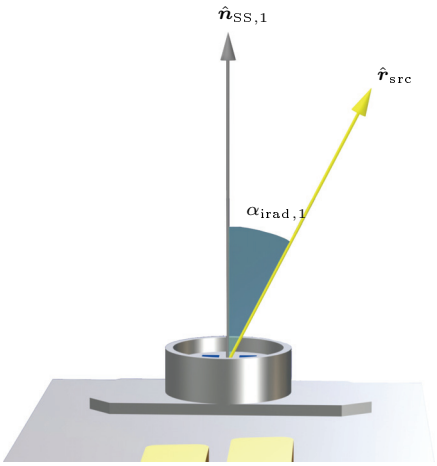

Figure 2. Definition of the angle of incidence $\alpha_{\mathrm{irad},j}$, illustrated on Sun sensor SS1 from the Ørsted satellite.

The parameter $i_{\max,j}$ may be assumed to scale linearly with the amount of incident irradiance. Hence the output generated from the solar irradiance is given by

$$i_{\mathrm{meas},j} = \frac{E_{\mathrm{irad}} i_{\max,j}}{E_{\mathrm{cal}}} \cos\left(\{\alpha_{\mathrm{irad},j}\}_{-\infty}^{\pi/2}\right), \tag{5}$$

where E_{irad} is the incident irradiance from an angle $\alpha_{\mathrm{irad},j}$ of incidence. Eq. (5) can be expressed in terms

of the Sun sensor normal vector $\hat{\boldsymbol{n}}_{\mathrm{SS},j}$ and the LOS vector to the source $\hat{\boldsymbol{r}}_{\mathrm{src}}$, as

$$i_{\mathrm{meas},j} = \frac{E_{\mathrm{irad}} i_{\mathrm{max},j}}{E_{\mathrm{cal}}} \left\{ \hat{\boldsymbol{n}}_{\mathrm{SS},j}^{\mathrm{T}} \hat{\boldsymbol{r}}_{\mathrm{src}} \right\}_0^{\infty}. \tag{6}$$

Eq. (6) is often used for estimating the output when disregarding the Earth albedo. In this case the incident irradiance is E_{AM0}, i.e. the solar irradiance at 1A.U. passing through zero air mass.

The total generated current in the Sun sensors is a sum of currents generated from the Sun irradiance, Earth albedo irradiance, and other fainter sources, which are assumed to be negligible. Recall from Eq. (3) that the output of the Earth albedo model is an array of albedo contributions from each cell in the partitioning of the Earth surface. This allows the Sun sensor output equation to include directional dependence to each cell, when calculating the current generated from Earth albedo. The interpretation of the Earth albedo array is illustrated in Fig. 3.

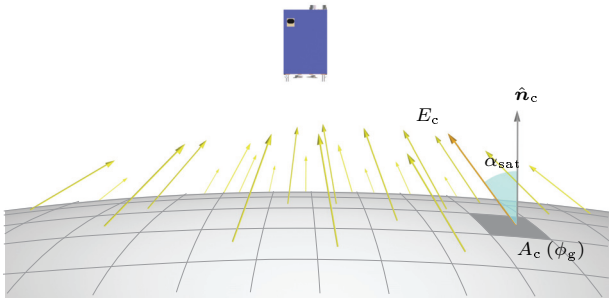

Figure 3. Albedo contributions in the Earth albedo model output. Each value in the albedo array is a irradiance contribution from a cell on the Earth surface.

The Earth albedo of a cell $E_{\mathrm{c}}(\phi_{\mathrm{g}}, \theta_{\mathrm{g}})$ is an irradiance contribution where the source is in the direction of the grid point $(\phi_{\mathrm{g}}, \theta_{\mathrm{g}})$ from the satellite. The Sun sensor output equation must calculate the contribution of each cell on the Sun sensor. The total generated current is calculated by summarizing the solar induced current and the contributions from each grid point. The resulting Sun sensor output equation becomes

$$i_{\mathrm{meas},j} = \frac{i_{\mathrm{max},j}}{E_{\mathrm{cal}}} \left(\left\{ E_{\mathrm{AM0}} \hat{\boldsymbol{n}}_{\mathrm{SS},j}^{\mathrm{T}} \hat{\boldsymbol{r}}_{\mathrm{Sun}} \right\}_0^{\infty} + \sum_{\boldsymbol{V}_{\mathrm{Sun}} \cap \boldsymbol{V}_{\mathrm{sat}}} \left\{ E_{\mathrm{c}}(\phi_{\mathrm{g}}, \theta_{\mathrm{g}}) \hat{\boldsymbol{n}}_{\mathrm{SS},j}^{\mathrm{T}} \hat{\boldsymbol{r}}_{\mathrm{g}} \right\}_0^{\infty} \right). \tag{7}$$

The $\hat{\boldsymbol{r}}_{\mathrm{g}}$ vector is the LOS vector from the satellite to the grid point $(\phi_{\mathrm{g}}, \theta_{\mathrm{g}})$.

Eq. (7) is a non-linear model of the current output of a Sun sensor. The attitude of the satellite, and consequently the Sun sensor, naturally influences the Sun sensor output. This dependency is included in the model, since the normal vector of the Sun sensor, $\hat{\boldsymbol{n}}_{\mathrm{SS},j}$, changes as the satellite rotates. The model incorporates the output of the Earth albedo model, which includes irradiance contributions from each cell of the partitioned Earth surface. This includes directional dependency of each cell irradiance. The Sun sensor model potentially allows improved Sun sensor vector observations and current simulation.

IV. Solar Vector Observation

Attitude determination is done by applying either a single-point algorithm or a filtering algorithm, see e.g. ([15,16]) for a description of the most common attitude determination algorithms. Filtering algorithms, such as the Kalman Filter, utilize models of the system and previous estimates of the satellite state, to predict the new state of the satellite. The prediction is compared to the measurements available, and a statistical optimal state estimate is calculated.[17] As opposed to filtering algorithms, the single-point algorithms solely use samples from a single time instant to estimate attitude. Common to most single-point algorithms is the

use of vector observations to estimate the attitude of an object. Given a set of $n \geq 2$ vector observations, a loss function is formulated, known as Wahba's problem, given by

$$L\left(\boldsymbol{A}_{\mathrm{I}}^{\mathrm{B}}\right) = \frac{1}{2}\sum_{j=1}^{n} w_j \left|\left|\hat{\boldsymbol{v}}_j^{\mathrm{B}} - \boldsymbol{A}_{\mathrm{I}}^{\mathrm{B}}\hat{\boldsymbol{v}}_j^{\mathrm{I}}\right|\right|^2, \tag{8}$$

where w_j is the weight of the j'th vector observation, $\hat{\boldsymbol{v}}_j^{\mathrm{I}}$ is the LOS vector in the reference frame, and $\boldsymbol{A}_{\mathrm{I}}^{\mathrm{B}}$ is the orthonormal rotation matrix, representing the rotation from reference to body frame, which is sought.[18] The loss function is the suare of a weighted sum of differences between the measured and the reference LOS vectors in the body frame. By minimizing the loss function, given in Eq. (8), an optimal attitude may be estimated.

One of the vector observations used to solve Wahba's problem are in many cases acquired from Sun sensors. These sensors result in a Sun LOS vector, available in a reference frame through ephemeris models, if absolute time and satellite orbit parameters are available. The measurement of this vector is error-prone if the Earth abledo is disregarded, as described in Section III. In the following the Sun sensor model will be utilized with the Earth albedo model in order to obtain a vector pair which is more accurate than the Sun LOS vector pair.

Sun sensors convert radiant flux to electrical power and can be used to estimate the angle between the normal vector to the sensor plane and the Sun LOS vector, by measuring the intensity per area on the sensor's solar cell surface, which is related to the angle of incident irradiance. Sun sensors are typically mounted such that measurements are available in six directions, opposite facing in pairs, ensuring that all of $\mathbb{R}^3$ is spanned. Typically a minimum of six Sun sensors are used, looking in the positive and negative directions of each axis in the spacecraft reference frame, as it is the case on the Ørsted satellite.[19] Without loss of generality it is assumed that six Sun sensor measurements are available, and that the Sun sensors are mounted looking in pairs of opposite directions, along orthogonal axes. If this is not the case, the measurements can be projected onto orthogonal axes, and the results will still apply.

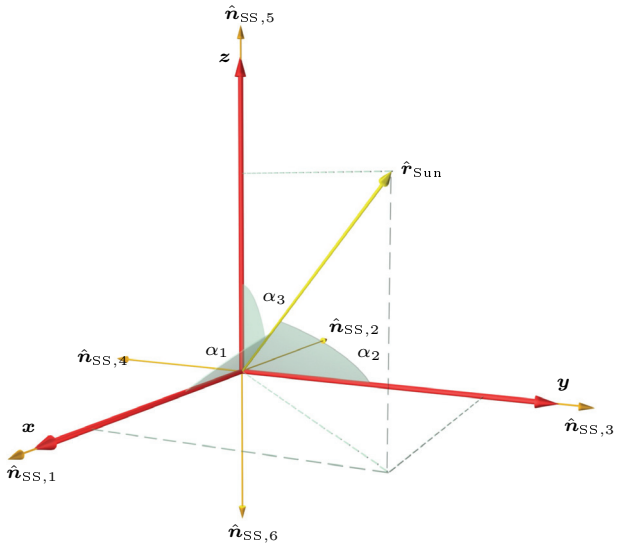

Figure 4. Projections of the Sun LOS vector measured by Sun sensors mounted in opposite looking directions along three orthogonal axes.

Fig. 4 shows the geometry of the Sun LOS vector $\hat{\boldsymbol{r}}_{\mathrm{Sun}}$ in a configuration, where six sun sensors are mounted in pairs in opposite directions and along three orthogonal axes. The Sun sensors are represented by the normal vectors $\hat{\boldsymbol{n}}_{\mathrm{SS},j}$ of each sensor SS1 through SS6. In the following section a standard algorithm of obtaining the Sun LOS vector is presented.

A. Standard Algorithm

Applying the cosine model of the Sun sensor current and normalizing the measured current $i_{\mathrm{meas},j}$, with respect to the maximum generated current $i_{\mathrm{max},j}$, i.e. when the incident light hits the Sun sensor orthogonally

onto the solar cells, the measurement can be written as

$$\frac{i_{\text{meas},j}}{i_{\text{max},j}} = \cos\left(\{\alpha_{\text{irad},j}\}_{-\infty}^{\pi/2}\right), \tag{9}$$

which is the projection of $\hat{\boldsymbol{r}}_{\text{Sun}}$ onto $\hat{\boldsymbol{n}}_{\text{SS},j}$. This is a simplified equation compared to the measurement model in Eq. (7), since it assumes a single constant irradiance source. However, this is the typical assumption used, since the solar irradiance may be assumed constant, and the Earth albedo is disregarded.

If the Sun sensor is looking in the negative direction of an axis, then Eq. (9) is the projection onto the associated axis in negative direction. The elements of the estimated Sun LOS vector, $\hat{\boldsymbol{r}}_{\text{SunEst}}$, may be written as

$$\frac{E_{\text{AM0}}}{E_{\text{cal}}}\hat{\boldsymbol{r}}_{\text{SunEst}} = \begin{bmatrix} \frac{i_{\text{meas},1}}{i_{\text{max},1}} - \frac{i_{\text{meas},2}}{i_{\text{max},2}} \\ \frac{i_{\text{meas},3}}{i_{\text{max},3}} - \frac{i_{\text{meas},4}}{i_{\text{max},4}} \\ \frac{i_{\text{meas},5}}{i_{\text{max},5}} - \frac{i_{\text{meas},6}}{i_{\text{max},6}} \end{bmatrix}. \tag{10}$$

Note that the resulting vector is scaled by the ratio between the incident irradiance and the calibrated irradiance. If the Sun sensor parameter $i_{\text{max},j}$ is calibrated using E_{AM0}, a unit vector is formed. The above equation is the standard algorithm for constructing a Sun LOS vector. This algorithm is error-prone when the Earth albedo induces currents in the Sun sensors. When observing a Sun sensor pair of opposite facing Sun sensors, the Earth albedo will either increase or decrease the estimate of the associated element of the $\hat{\boldsymbol{r}}_{\text{SunEst}}$ vector. If the solar irradiance and the Earth albedo illuminate the same Sun sensor, the estimated element will be too large. If opposite Sun sensors in the sensor pair are illuminated, the estimated element will be decreased, due to the subtraction of the currents in Eq. (10).

B. Summarized Sun and Earth Algorithm

The Summarized Sun and Earth (SSE) algorithm incorporates a simplification of the Earth albedo in the Sun sensor output equation in Eq. (7). The Earth albedo is approximated by a single vector, as opposed to contributions from each data point $(\phi_{\text{g}}, \theta_{\text{g}}) \in \boldsymbol{V}_{\text{Sun}} \cap \boldsymbol{V}_{\text{g}}$. The Earth albedo is assumed to reach the satellite anti-parallel to the Nadir vector. The approximated total Earth albedo irradiance, E_{a}, is calculated as the sum of irradiance contributions from all cells in the Earth albedo model, given by

$$E_{\text{a}} = \sum_{\boldsymbol{V}_{\text{Sun}} \cap \boldsymbol{V}_{\text{sat}}} E_{\text{c}}\left(\phi_{\text{g}}, \theta_{\text{g}}\right). \tag{11}$$

With this assumption, the output equation of the Sun sensors can be approximated by

$$i_{\text{meas},j} = \frac{i_{\text{max},j}}{E_{\text{cal}}}\left(\left\{E_{\text{AM0}}\hat{\boldsymbol{n}}_{\text{SS},j}^{\text{T}}\hat{\boldsymbol{r}}_{\text{Sun}}\right\}_0^{\infty} + \left\{E_{\text{a}}\hat{\boldsymbol{n}}_{\text{SS},j}^{\text{T}}\hat{\boldsymbol{r}}_{\text{E}}\right\}_0^{\infty}\right), \tag{12}$$

where $\hat{\boldsymbol{r}}_{\text{E}}$ is the Nadir vector. With the above approximation, and applying the standard Sun LOS vector algorithm in Eq. (10), the resulting estimated vector is actually the sum of the Sun and Earth irradiance vectors, i.e.

$$\frac{1}{E_{\text{cal}}}\left(E_{\text{AM0}}\hat{\boldsymbol{r}}_{\text{Sun}} + E_{\text{a}}\hat{\boldsymbol{r}}_{\text{E}}\right) = \begin{bmatrix} \frac{i_{\text{meas},1}}{i_{\text{max},1}} - \frac{i_{\text{meas},2}}{i_{\text{max},2}} \\ \frac{i_{\text{meas},3}}{i_{\text{max},3}} - \frac{i_{\text{meas},4}}{i_{\text{max},4}} \\ \frac{i_{\text{meas},5}}{i_{\text{max},5}} - \frac{i_{\text{meas},6}}{i_{\text{max},6}} \end{bmatrix}. \tag{13}$$

The SSE vector is shown in Fig. 5. The SSE vector is an improved estimate of the vector projected onto the axes spanned by the Sun sensors, as opposed to the Sun LOS vector of the Standard algorithm, shown in Fig. 4.

The proof of Eq. (13) is given for the first element of the vector. An expression of the first element can be found by inserting Eq. (12) into Eq. (13),

$$\frac{i_{\text{meas},1}}{i_{\text{max},1}} - \frac{i_{\text{meas},2}}{i_{\text{max},2}} = \frac{1}{E_{\text{cal}}}\left(\left\{E_{\text{AM0}}\hat{\boldsymbol{n}}_{\text{SS},1}^{\text{T}}\hat{\boldsymbol{r}}_{\text{Sun}}\right\}_0^{\infty} + \left\{E_{\text{a}}\hat{\boldsymbol{n}}_{\text{SS},1}^{\text{T}}\hat{\boldsymbol{r}}_{\text{E}}\right\}_0^{\infty} - \left\{E_{\text{AM0}}\hat{\boldsymbol{n}}_{\text{SS},2}^{\text{T}}\hat{\boldsymbol{r}}_{\text{Sun}}\right\}_0^{\infty} - \left\{E_{\text{a}}\hat{\boldsymbol{n}}_{\text{SS},2}^{\text{T}}\hat{\boldsymbol{r}}_{\text{E}}\right\}_0^{\infty}\right). \tag{14}$$

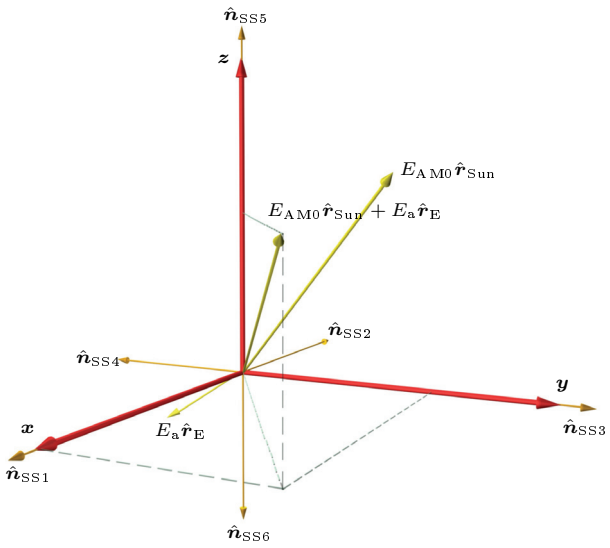

Figure 5. Projections of the SSE vector measured by Sun sensors mounted in opposite looking directions along three orthogonal axes.

Since the Sun sensor pair SS1 and SS2 are facing opposite directions, it holds that

$$\hat{\boldsymbol{n}}_{\mathrm{SS},1} = -\hat{\boldsymbol{n}}_{\mathrm{SS},2}. \tag{15}$$

As a result the saturation function on the Sun irradiance vector can be eliminated by

$$\left\{E_{\mathrm{AM0}}\hat{\boldsymbol{n}}_{\mathrm{SS},1}^{\mathrm{T}}\hat{\boldsymbol{r}}_{\mathrm{Sun}}\right\}_0^{\infty} - \left\{E_{\mathrm{AM0}}\hat{\boldsymbol{n}}_{\mathrm{SS},2}^{\mathrm{T}}\hat{\boldsymbol{r}}_{\mathrm{Sun}}\right\}_0^{\infty} = \left\{E_{\mathrm{AM0}}\hat{\boldsymbol{n}}_{\mathrm{SS},1}^{\mathrm{T}}\hat{\boldsymbol{r}}_{\mathrm{Sun}}\right\}_0^{\infty} + \left\{E_{\mathrm{AM0}}\hat{\boldsymbol{n}}_{\mathrm{SS},1}^{\mathrm{T}}\hat{\boldsymbol{r}}_{\mathrm{Sun}}\right\}_{-\infty}^{0} \tag{16}$$

$$= E_{\mathrm{AM0}}\hat{\boldsymbol{n}}_{\mathrm{SS},1}^{\mathrm{T}}\hat{\boldsymbol{r}}_{\mathrm{Sun}}. \tag{17}$$

The same applies for the Earth irradiance vector. Inserting into Eq. (14), yields

$$\frac{i_{\mathrm{meas},1}}{i_{\mathrm{max},1}} - \frac{i_{\mathrm{meas},2}}{i_{\mathrm{max},2}} = \frac{1}{E_{\mathrm{cal}}}\left(E_{\mathrm{AM0}}\hat{\boldsymbol{n}}_{\mathrm{SS},1}^{\mathrm{T}}\hat{\boldsymbol{r}}_{\mathrm{Sun}} + E_{\mathrm{a}}\hat{\boldsymbol{n}}_{\mathrm{SS},1}^{\mathrm{T}}\hat{\boldsymbol{r}}_{\mathrm{E}}\right), \tag{18}$$

or equivalently

$$\frac{i_{\mathrm{meas},1}}{i_{\mathrm{max},1}} - \frac{i_{\mathrm{meas},2}}{i_{\mathrm{max},2}} = \frac{\hat{\boldsymbol{n}}_{\mathrm{SS},1}^{\mathrm{T}}}{E_{\mathrm{cal}}}\left(E_{\mathrm{AM0}}\hat{\boldsymbol{r}}_{\mathrm{Sun}} + E_{\mathrm{a}}\hat{\boldsymbol{r}}_{\mathrm{E}}\right), \tag{19}$$

which is the first element of the SSE irradiance vector, since $\hat{\boldsymbol{n}}_{\mathrm{SS},1}$ is aligned with the $\boldsymbol{x}$ axis, illustrated in Fig. 5.

Eq. (19) shows that the vector formed from the Sun sensors is actually not the Sun LOS vector, but a summarized Sun and Earth vector, scaled by the amount of direct solar irradiance and Earth albedo irradiance. If the measured vector is paired with the Sun LOS reference vector, errors are introduced in the attitude determination, when solving Wahba's problem in Eq. (8), since it is not the same vector, which is represented in the two frames. In order to calculate the correct reference vector, the Earth albedo model must be utilized. Using the approximated Sun sensor model, which uses the total Earth albedo irradiance output from the Earth albedo model, this reference vector may be calculated, thus improving the performance of all attitude determination algorithms based on solar vector observations.

V. Results

In this section the Earth albedo model and Sun sensor model is compared with telemetry data from the Danish Ørsted satellite. The simulations are done in Simulink, which is a graphical user interface to

Matlab from The Mathworks. The Earth albedo model is implemented in Matlab with a Simulink interface. The implementation is released as the Earth Albedo Toolbox and may be freely downloaded at the author's website.[20]

The Ørsted satellite is equipped with Sun sensors, and since the orbit and attitude of the satellite is known, the Earth albedo model can be applied in order to estimate the currents from the Sun sensors. These estimates are then compared to the sampled currents in the telemetry data, in order to validate the Earth albedo modeling algorithm.

The Danish Ørsted satellite was launched on February 23, 1999 into Low Earth Orbit (LEO). The main scientific mission is a precise global mapping of the Earth's magnetic field. The Ørsted satellite is equipped with two magnetometers, the Compact Spherical Coil (CSC) flux-gate and Overhauser magnetometers, for measuring the magnetic field magnitude and direction. The Ørsted satellite is characterized by its eight meter boom, at the end of which the CSC flux-gate magnetometer is placed, in order to minimize electromagnetic disturbances from the on-board electronics. Also on the boom, at a distance of six meters from the main body of the satellite, a star imager is mounted. This allows for attitude measurements with an accuracy between 5 to 20as.[11,21] An illustration of the Ørsted satellite is shown in Fig. 6.

Figure 6. Illustration of the Ørsted satellite.

The Ørsted satellite is equipped with eight Sun sensors, two three axis and two single axis. Fig. 7 shows the placement of the sensors in the spacecraft body frame. This configuration results in redundant measurements of the incident irradiance in positive and negative $\boldsymbol{z}_{\mathrm{SCB}}$ directions.

The Ørsted satellite telemetry data is down-linked when the satellite is above the ground station in Copenhagen, Denmark. The data packet utilized in the validation is from May 21, 2001, which is telemetry data packet 5200. The total time of which data from the Star Imager and Attitude Control System (ACS) house keeping data are available is 3:52:03.707 PM to 10:10:16.469 PM. The telemetry data is used in conjunction with reference models implemented in Simulink. The ephemeris models are based on a Special General Perturbation Model of Fourth Order (SGP4) orbital propagator. The Sun sensor model is calibrated with respect to solar cell efficiency degradation, star tracker misalignment due to boom deployment discrepancies, and temporal discrepancies due orbit parameter uncertainty. Temperature compensation has also been investigated and has been included in the modeling of Sun sensors. The influence of the temperature variation on the solar cell efficiencies in the Sun sensors has negligible impact on the output accuracy, hence it is not presented.

The resulting simulation of the Sun sensor currents, disregarding Earth albedo, is plotted with the Ørsted telemetry in Fig. 8. The simulated currents are calculated from the solar irradiance only, which

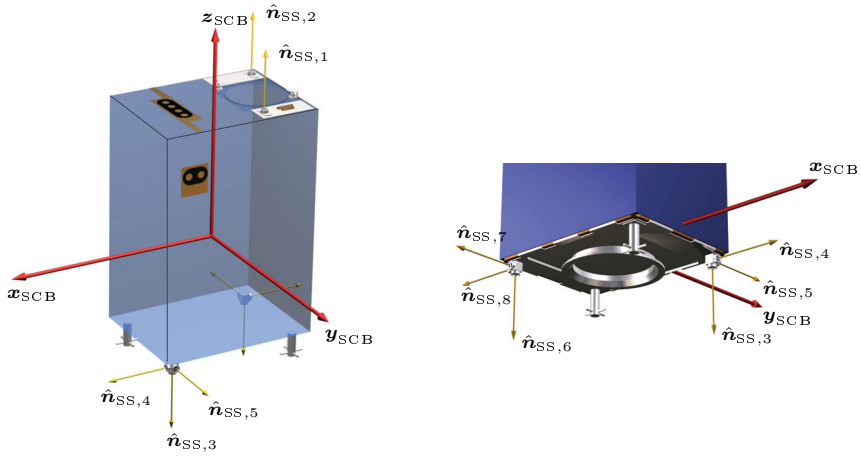

(a) Top View (b) Bottom View

Figure 7. Placement of the Ørsted Sun sensors in the spacecraft reference frame. The boom extends in the positive z_{SCB} direction.

is why additional currents are seen on a number of the Sun sensors. These currents are generated by the Earth albedo. The deviation of the current in Sun sensor SS1 is due to shading from the boom, which is not considered in the Sun sensor model. Additionally it should be noted that SS7 has been identified as faulty, due to an suspected crack in the cover glass of the sensor.

Fig. 9 shows the calibrated currents including the Earth albedo induced currents, calculated using the Earth albedo model. The Earth albedo model uses the TOMS reflectivity data from the day of the orbit. Table 1 lists the RMS errors in the current simulation when compared to the measured Sun sensor currents in the Ørsted telemetry.

Table 1. RMS errors of the Sun sensor current estimation, with and without using the Earth albedo model.

Sun Sensor	RMS Error [mA] wo. Albedo Comp.	RMS Error [mA] w. Albedo Comp.
SS1	0.193	0.193
SS2	0.062	0.062
SS3	0.175	0.060
SS4	0.063	0.058
SS5	0.041	0.020
SS6	0.184	0.053
SS7	0.121	0.105
SS8	0.043	0.039

It can be seen from the plots that the Earth albedo model and Sun sensor model are able to estimate the additional Earth albedo induced currents. Since Sun sensors SS3 and SS6 are Nadir pointing Sun sensors, due to the gravity gradient stabilization of the satellite, the albedo currents are most apparent on these sensors. The RMS errors of the current simulation are reduced from 0.18mA to 0.053mA. It is seen that even though Sun sensors SS4, SS5, SS7, and SS8 are perpendicular to the Nadir vector, due to the gravity stabilization of the satellite, the simulation is able to estimate Earth albedo currents on these panels also, thus showing the significance of maintaining directional information in the Earth albedo modeling. It is

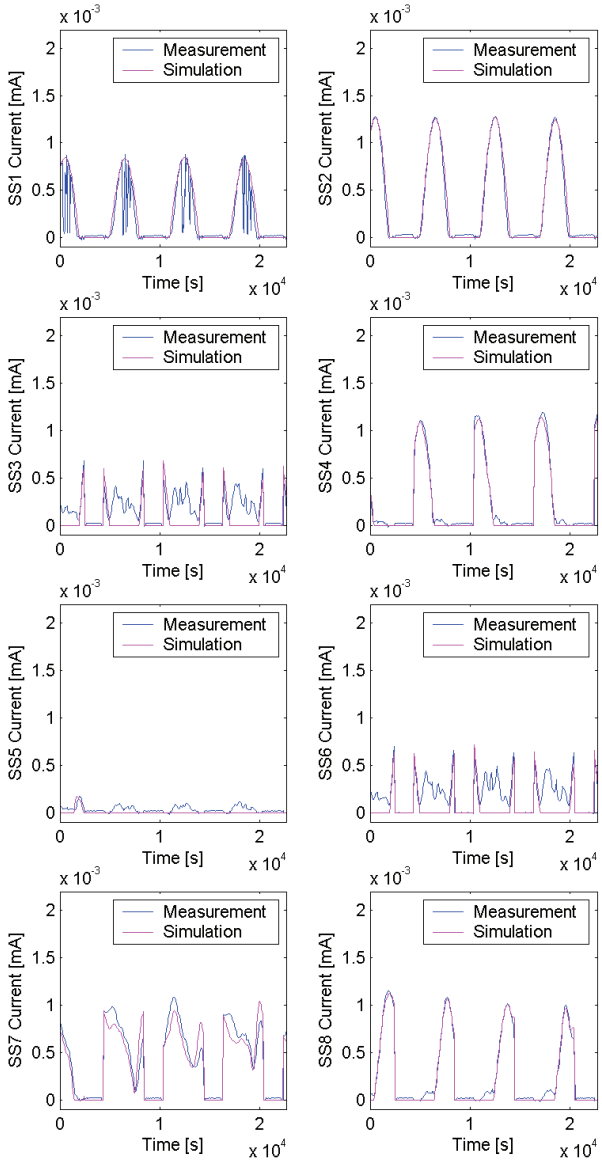

Figure 8. Measured and simulated currents of the eight solar cells on the Ørsted satellite after calibration of the solar cell efficiencies.

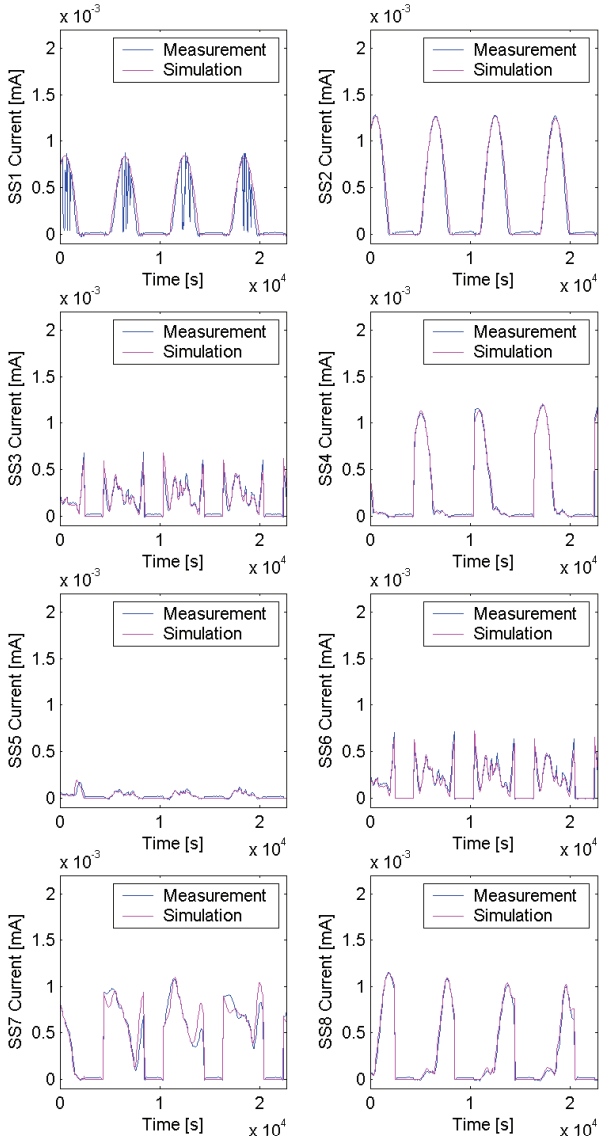

Figure 9. Measured currents of the eight solar cells on the Ørsted satellite with the simulated current using the albedo model and daily reflectivity data.

clearly seen that the Earth albedo model in conjunction with the Sun sensor model in Eq. (7) can be applied in the modeling of the irradiance of the Earth albedo and the resulting generated currents in photo voltaics.

The errors on the Sun LOS vector observation from the Ørsted satellite telemetry data can be compared to the reference model. The vector observations are the input to the attitude determination algorithm, and therefore the precision of these measurements directly influence the performance of the algorithms. The results of the SSE algorithm is compared to the Standard algorithm.

In order to compare the Ørsted Sun LOS vector observation with the reference model, the star tracker telemetry is used to obtain the reference vectors in the SCB frame. The Sun sensor currents are processed in order to obtain the SSE irradiance vector, using the algorithm described in Section IV. The resulting vector is compared with the Sun LOS vector and the SSE vector from the ephemeris model. Fig. 10 shows the angular separation between the vector pairs, and Table 2 shows the resulting Root-Mean-Square (RMS) errors. The RMS separation between the SSE vectors is 6.9 deg. The RMS angular separation of the measured vector observation, when compared to the Sun LOS vector is 11 deg.

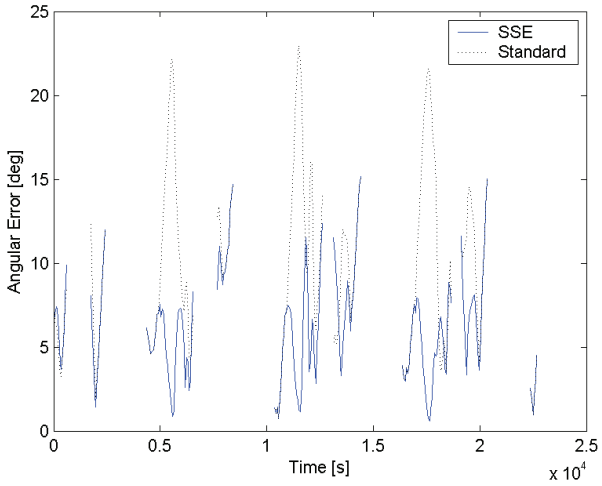

Figure 10. Angular separation between the SSE vector pair, compared with the Sun LOS vector observation without albedo compensated reference vector.

Table 2. Statistics of the Sun sensor vector pairs.

Algorithm	RMS Error [deg]
Standard	11.2
SSE	6.93

VI. Conclusion

An Earth albedo model based on TOMS reflectivity data was derived in ([10]). The Earth albedo model calculates the albedo contribution of 180×288 cells in a partitioning of the Earth surface, thus maintaining directional information of the incident albedo irradiance. In this paper, the Earth albedo model has been included in a Sun sensor model, in order to predict the amount of Earth albedo induced current. It was proven that the vector formed from the Sun sensors by standard methods is a summarized vector of the Sun and Earth albedo irradiances. By utilizing the Earth albedo model, this vector may be calculated in the reference frame, yielding a vector pair which is more accurate when applied in the solving of Wahba's problem for attitude determination.

The proposed model has been verified by including the Earth albedo model in a Sun sensor current model, and comparing the simulation results with telemetry from the Ørsted satellite. The resulting simulation error of the Sun sensor currents is improved from 0.18mA RMS to 0.053mA. This significant improvement of the Sun sensor current simulation validates the Earth albedo model and the Sun sensor current model, in which

the Earth albedo model is utilized. Additionally, it is shown that the angular separation between the Sun sensor vector observation and associated reference vector is improved from 11.2deg to 6.93deg, when utilized with the summarized Sun and Earth albedo irradiance vector, as opposed to the Sun LOS vector. This result is important when utilizing Sun sensors in solving Wahba's problem in order to calculate the attitude of a satellite.

A. Future Work

The Earth albedo model has been successfully validated, and a method for obtaining improved solar-based vector observation has been presented. Since the vector observation is actually a sum of two irradiance sources, observability is added to the system. This indicates that it is possible to perform three-axis attitude determination using only Sun sensors. Investigation in such algorithms is currently in progress. Due to the highly non-linearity of the Sun sensor model, a single-point algorithm is not trivially derived. Genetic algorithms could be considered for such application. Considering filtering methods, a problem arises due to the non-differentiability of the output equation. One such way of handling this problem, is by applying Unscented Kalman Filtering. Using the Unscented Kalman Filter allows estimation of satellite attitude and angular rate using only Sun sensors.

References

[1]Harris, M. and Lyle, R., "Spacecraft Radiation Torques," Tech. Rep. NASA SP-8027, National Aeronautics and Space Administration, October 1969.

[2]Wertz, J. R., editor, *Spacecraft Attitude Determination and Control*, Kluwer Academic Publishers, 1978.

[3]Wertz, J. R., editor, *Mission Geometry: Orbit and Constellation Design and Management*, Microcosm Press AND Kluwer Academic Publishers, 2001.

[4]Hales, J. H. and Pedersen, M., "Two-axis MOEMS Sun Sensor for Pico Satellites," *16th Annual AIAA/USU Conference on Small Satelites*, August 2001.

[5]Brasoveanu, D. and Sedlak, J., "Analysis of earth albedo effect on sun sensor measurements based on theoretical model and mission experience," *AAS/GSFC 13th International Symposium on Space Flight Dynamics*, Vol. 1, May 1998, pp. 435–447.

[6]Humphreys, T. E., "Attitude Determination for Small Satellites with Modest Pointing Constraints," *AIAA Student Conference on Small Satellites*, August 2002.

[7]Psiaki, M. L., Martel, F., and Pal, P. K., "Three-Axis Attitude Determination via Kalman Filtering of Magnetometer Data," *Journal of Guidance, Control, and Dynamics*, Vol. 13, No. 3, May-June 1990, pp. p. 506–514.

[8]van Beusekom, C. J. and Lisowski, R., "Three-Axes Attitude Determination for Falconsat-3," *AIAA Student Conference*, April 2003.

[9]Fisher, H. L., Musser, K. L., and Shuster, M. D., "Coarse attitude determination from Earth albedo measurements," *IEEE Transactions on Aerospace and Electronic Systems*, 1993.

[10]Bhanderi, D. D. V. and Bak, T., "Modeling Earth Albedo for Satellites in Earth Orbit," *AIAA Guidance, Navigation, and Control Conference*, August 2005.

[11]Liebe, C. C., "Star Trackers for Attitude Determination," *IEEE Aerospace and Electronic Systems Magazine*, Vol. 10, No. 6, 1995, pp. 10–16.

[12]Mazer, J. A., *Solar Cells: An Introduction to Crystalline Photovoltaic Technology*, Kluwer Academic Publishers, 1997.

[13]Ryer, A., *Light Measurement Handbook*, International Light, 1997.

[14]Emcore, "InGaP/GaAs/Ge Tripple-Junction Solar Cells," Technical specification, EMCORE, 2004.

[15]Lerner, G. M., *Spacecraft Attitude Determination and Control*, chap. Three-Axis Attitude Determination, D. Reidel, Dordrecht, The Netherlands, 1978, pp. 420–428.

[16]Markley, F. L., Crassidis, J. L., and Cheng, Y., "Nonlinear Attitude Filtering Methods," *AIAA Guidance, Navigation, and Control Conference*, August 2005.

[17]Grewal, M. S. and Andrews, A. P., *Kalman Filtering Theory and Practice*, Prentice Hall, 1993.

[18]Wahba, G., "A Least Squares Estimate of Satellite Attitude," *SIAM Review*, Vol. 7, No. 3, July 1965, pp. 409–426.

[19]Blanke, M., Wisniewski, R., and Caspersen, G., "Sun Sensor System Requirements," Tech. rep., Aalborg University, April 1994.

[20]Bhanderi, D. D. V., http://bhanderi.dk/, 2006.

[21]Jørgensen, J. L., "Development of the Ørsted Precision Attitude Instrument the Star Imager," *The Chapman Conference on Measurement Techniques for Space Plasmas*, 1995.